Bioprinting 12 (2018) e00037

Contents lists available at ScienceDirect

Bioprinting

journal homepage: www.elsevier.com/locate/bprint

Commercially available microgels for 3D bioprinting

Christopher S. O'Bryan[a], Tapomoy Bhattacharjee[a], Samantha L. Marshall[a], W. Gregory Sawyer[a,b], Thomas E. Angelini[a,c,d,*]

[a] Department of Mechanical & Aerospace Engineering, University of Florida, Gainesville, FL, United States
[b] Department of Materials Science and Engineering, University of Florida, Gainesville, FL, United States
[c] J. Crayton Pruitt Family Department of Biomedical Engineering, University of Florida, Gainesville, FL, United States
[d] Institute for Cell & Tissue Science and Engineering, University of Florida, Gainesville, FL, United States

ARTICLE INFO

Keywords:
Bioprinting
3D Printing
Sacrificial supports
Microgels
Soft matter manufacturing

ABSTRACT

One of the major limitations in 3D bio-printing technology is the lack of materials capable of providing stable mechanical support to extremely soft and delicate structures; cells and biopolymers deform, disperse, and behave unpredictably without additional support. 3D printing into jammed solids made from soft microgel particles was shown recently to solve many of the problems of printing with these extremely challenging materials. However, this approach was tested with only a limited number of microgel systems, limiting its potential application to diverse problems. Here we test the robustness of 3D printing into several different, chemically distinct jammed microgel materials. We find that the rheological behavior of each system can be tuned to achieve high-precision 3D printing of numerous structures, with the freedom to choose different path planning strategies and writing nozzle design.

1. Introduction

Advanced tissue engineering now employs additive manufacturing techniques for 3D printing with living cells, natural extracellular matrix, and synthetic hydrogels [1,2]. These materials provide practically no physical support to the printed structures that they constitute, which has led to the development of complex reinforcement strategies and specially designed bio-inks [3–6]. Once printed, soft biomaterial structures are delicate and require extremely gentle processing steps to be removed from their supporting matrix. Accordingly, such delicate hydrogels and cell-laden scaffolds are often toughened chemically or mechanically to improve their functionality [7,8]. An alternative, purely physical strategy has recently been developed that leverages the microgel jamming transition to preserve structures by trapping material in space with a demonstrated precision of 1–2 cell diameters [9–11]. This approach to structuring non-self-supporting materials with high precision and few restrictions on material selection has been tested with hydrogels, extracellular matrix, and living cells. However, only a limited number of microgel system have been investigated [10–12]; microgel materials vary widely in their polymer-solvent interactions and in crosslinking and charge densities. If jammed granular microgel systems are to be useful throughout biomanufacturing, the same rheological behavior for controlled 3D bioprinting must be achievable in chemically distinct microgel systems.

In this letter, we investigate the effects of chemical composition on the precision of 3D printing into granular microgels. We find that four chemically different, commercially available microgel systems can be tuned to exhibit similar rheological behaviors. In all cases, the resulting materials perform comparably in 3D printing tests, in which a 20–50 μm feature size is achieved.

2. Methods and materials

2.1. Microgel preparation

Rheological testing and 3D printing experiments are conducted using four commercially available microgels: Carbopol ETD 2020, Carbopol 980-NF, Carbopol Ultrez 20, and Pemulen TR-2NF. Microgels samples are prepared at various concentrations in ultrapure water (18.2 MΩ×cm) and homogenized by speed mixing at 3500 rpm for 15 min. Microgels are swollen to jamming by adding 10N NaOH until a pH of 6.0 is achieved. Jammed microgel samples are speed mixed for 1 min at 3000 rpm to remove trapped air bubbles prior to use.

2.2. Rheological characterization

Rheological measurements are performed on a Malvern Kinexus Pro+ rheometer using a roughened 40 mm cone with an angle of 4° and

* Corresponding author at: Department of Mechanical & Aerospace Engineering, University of Florida, Gainesville, FL, United States.
E-mail address: t.e.angelini@ufl.edu (T.E. Angelini).

https://doi.org/10.1016/j.bprint.2018.e00037
Received 1 August 2018; Received in revised form 10 October 2018; Accepted 26 October 2018

a roughened 40 mm lower plate. Low amplitude frequency sweeps are performed at 1% strain ranging from 10^{-3} to 10^{0} Hz. Unidirectional shear rate sweeps are conducted between from 500 to 10^{-3} s^{-1}. The thixotropic time of the material is measured by applying a 100 Pa stress to the material for 30 s and subsequently reducing the stress to 1/10 the yield stress of the material.

2.3. Cell viability studies

Cell viability studies are performed using 3T3 Fibroblast cells cultured in DMEM cell growth media containing L-Glutamine, 4.5 g/L Glucose, and Sodium Pyruvate (Corning) and supplemented with 10% Fetal Bovine Serum (Corning) and 1% Penicillin Streptomycin (Gibco). Live cells are dyed using CellTracker Green CMFDA (Invitrogen) and dead cells are dyed using ethidium homodimer (Invitrogen). Fluorescence images are captured using a Nikon C2+ Confocal microscope and analyzed using FIJI ImageJ software.

2.4. 3D printing

3D printing into jammed granular microgels is performed using three linear translation stages (Newport) with an attached linear stage as a syringe pump (Physik Instrumente). Polyvinylalcohol polymer containing approximately 1% (w/w) fluorescent microspheres is loaded into a syringe (Hamilton) equipped with a disposable blunt dispensing needle (Vita Needle). Both the syringe pump and translation stages are controlled through custom written MATLAB scripts.

3. Results and discussion

3D printing into jammed granular microgels is possible because the stress generated by an immersed, translating injection tip can locally yield the surrounding material, allowing a second material to be left along its path [10]. As the injection tip leaves the printing region, the microgels will spontaneously and rapidly jam into a dominantly solid-like state, trapping the created structures in place (Fig. 1a). The microgels used here are granular in size ($d > 1\,\mu m$) to eliminate thermally driven Brownian motion of the particles, providing stability to printed structures [13]. We prepare the microgel systems at high packing densities to ensure that the system is jammed when left unperturbed (Fig. 1b). Highly swelled microgels achieve this packing density at low polymer concentration, reducing osmotic pressure on the printed material with increased polymer mesh-size, ξ (Fig. 1c-d). For printing with biological materials like cells, this low osmotic pressure prevents compression of cell bodies and allows diffusion of small nutrient and waste molecules. Microgels prepared in this way exhibit the rheological properties of soft elastic solids at low applied stresses and flow like viscous fluids at high applied stresses (Fig. 1e-f). We term these materials *Liquid Like Solids* (LLS) to reflect this essential combination of rheological properties.

To determine whether the rheology of chemically distinct LLS materials can be utilized for 3D printing, we investigate four different, commercially available microgel systems in search of rheological properties favorable for 3D bioprinting, notably a low elastic modulus (≈100 Pa) and yield stress (≈10 Pa), dominant elastic behavior, and rapid recovery of this elastic behavior after yielding (≈1 s). Here, we focus our investigation on Carbopol ETD 2020, Carbopol 980-NF, Carbopol Ultrez 20, and Pemulen TR-2NF. These materials are composed of acrylic acid with varying charge densities, crosslinking densities, and functional groups that provide different swelling behavior. Briefly: ETD 2020 and Ultrez are copolymers consisting of acrylic acid and C10-C30 alkyl acrylate that have been hydrophobically-modified with a PEG-*block*-alkyl acid ester copolymer whereas 980-NF is a crosslinked polyacrylic acid with no additional functional

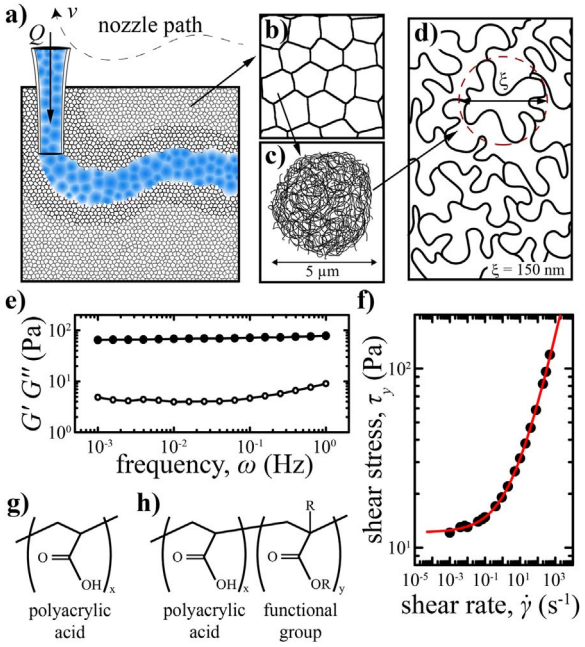

Fig. 1. Characterization of Liquid Like Solids. (a) The localized fluidization of LLS enables 3D printing of soft biomaterials. (b) LLS materials are formed from jammed microgels. (c) The microgels used here are hydrogel particles approximately 5 μm in diameter. (d) The large mesh-size within these microgels allows the diffusion of small molecules. (e) Frequency sweeps at 1% strain show rheological characteristics of soft elastic solids (f) Shear rate sweeps exhibit a plateau in shear stress at low shear rates, corresponding to the yield stress. Applied stress above the yield stress fluidizes the LLS as the microgels transition from the jammed to the unjammed state. (g) Chemical structure of Carbopol 980-NF, a crosslinked polyacrylic acid with no additional functional group. (h) General chemical structure of Carbopol ETD 2020, Carbopol Ultrez 20, and Pemulen TR-2NF. These microgels consist of a copolymer of polyacrylic acid and a C10-C30 alkyl acrylate functional group.

groups (Fig. 1g,h) [14,15]. Pemulen is a copolymer consisting of acrylic acid and C10-C30 alkyl acrylate crosslinked with allyl pentaerythritol and modified to provide emulsifying properties [16,17]. We hypothesize that these differences will change the swelling behavior of the microgels, thereby re-scaling the concentration dependence rheological performance. To explore these changes in rheological performance, we test all four systems over a wide concentration range.

To characterize the rheological behavior of the various microgels, we perform low amplitude frequency sweeps, covering a range of 10^{-3} to 10^{0} Hz, measuring the elastic modulus (G') and viscous modulus (G''). We find that for all four systems, G' and G'' remain relatively flat and separated across the spectrum of oscillatory frequencies, behaving like linear solids with damping (Fig. 2a). Recently, differences between these materials in their charge density were found through analyzing the scaling relationships between their moduli and concentrations [18]. Here, we find that Ultrez, 980-NF, and Pemulen follow scaling concentration scaling behavior consistent with low charge density polymers ($G' \sim c^{9/4}$) whereas the ETD 2020 scaling is consistent with high charge density polymers ($G' \sim c^{1.0}$), where c is the microgel polymer concentration (Fig. 2b). We show data from samples that exhibited favorable 3D printing performance, including a low elastic shear modulus (G' of 20–100Pa) and dominant elastic behavior over all frequencies (Fig. 2a). Thus, the chemical differences between these different microgels do not alter their qualitative rheological behavior and their linear behaviors can be tuned by controlling the polymer concentration.

Low yield stress and short thixotropic time of LLS materials are essential for their use in 3D printing to localize yielding and promote rapid re-flow and solidification of the granular microgel. The yield

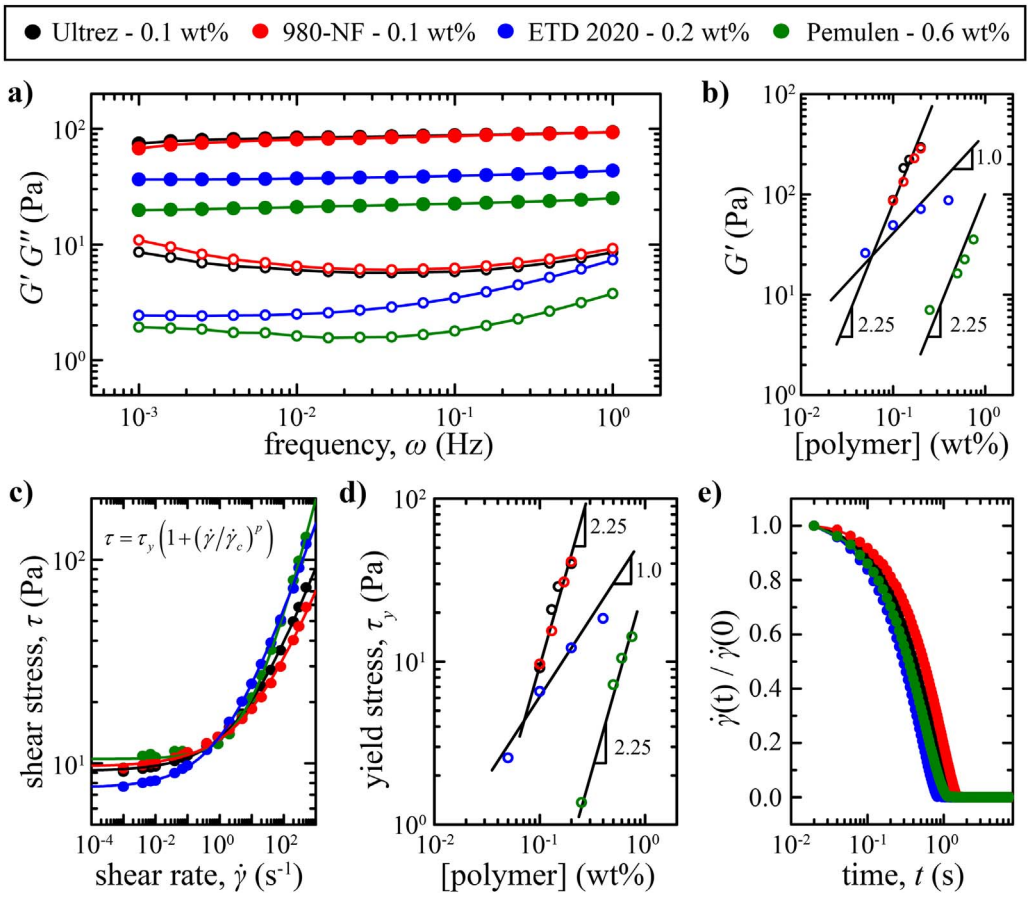

Fig. 2. Rheological characterization of chemically distinct LLS materials. Frequency sweeps are performed on four different microgel materials at 1% strain to measure the elastic (G') and viscous (G'')shear moduli. (a) At concentrations favorable for 3D printing, G' remains flat and separated from the G'', a characteristic of soft elastic solids. (b) For all four materials, G' increases with increasing polymer concentration. Ultrez, 980-NF, and Pemulen exhibit scaling behavior consistent with low charge density polyelectrolytes ($c^{9/4}$) while ETD 2020 follows the scaling behavior of high charge density ($c^{1.0}$). To study the transition between solid and fluidized behaviors, a shear rate sweep is performed and the Hershel-Bulkley model is fit to the data. (c) We find that all four commercially available microgels can be tuned to have a yield stress favorable for 3D bioprinting (~10 Pa). (d) The yield stress of the material can be tuned through changes to the polymer concentration. (e) The thixotropic time is determined by measuring the shear rate over time after dropping the applied stress to 1/10 the yield stress.

stress, τ_y of LLS is determined from a unidirectional shear rate sweep where shear stress is measured at progressively decreasing shear strain rates. As the shear rate, $\dot{\gamma}$ is ramped down to 10^{-3} s^{-1}, the measured stress becomes independent of the applied shear rate. This plateau stress is the yield stress of the LLS and can be determined by fitting the Herschel-Bulkley model, $\tau = \tau_y(1 + (\dot{\gamma}/\dot{\gamma}_c)^p)$, where $\dot{\gamma}_c$ is the crossover shear rate between regimes of behavior, and p is a dimensionless constant of order 0.5 (Fig. 2c) [19]. Here, we measure the yield stress of each microgel system at various concentrations (Fig. 2d). We find that all four chemically distinct microgel systems have a narrow range of yield stresses between 7 and 10 Pa at concentrations favorable for 3D printing (Fig. 2c).

The time it takes for a yielded material to spontaneously re-solidify after the applied stress drops below the yield stress is the thixotropic time. For 3D bioprinting into jammed granular microgels, this sets the time-scale in which materials become trapped once the printing nozzle has left the printing area. We measure the thixotropic time of jammed microgels by observing the shear rate response as the shear stress is dropped from 100 Pa to 1/10 the yield stress of the system; the point at which the shear rate plateaus and approaches zero is the thixotropic time of the system. We find all four microgel systems exhibit thixotropic times of order 1 s at the previously described concentrations (Fig. 2e).

To explore the application of LLS as a support material for 3D bioprinting, we perform short-term cell viability studies of cells cultured

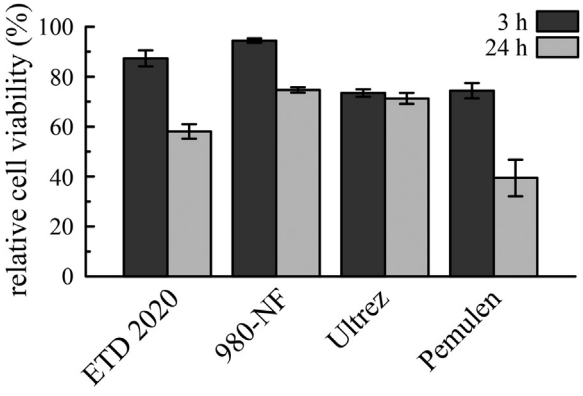

Fig. 3. Short-term cell viability studies of 3T3 fibroblast cells dispersed in microgel samples swollen in cell growth media relative to liquid growth media.

in microgel media. 3T3 fibroblast cells are dispersed in microgels swollen in cell growth media with the rheological properties previously described. We find that the LLS result in a reduced cell viability relative to cells cultured in liquid cell growth media (Fig. 3). Interestingly, microgels that have been hydrophobically modified with additional functional groups, *i.e.* ETD 2020, Ultrez, and Pemulen, demonstrate lower cell viability compared to the non-functionalized 980-NF. Previous studies have shown that viability is increased in cells cultured in ETD 2020 when

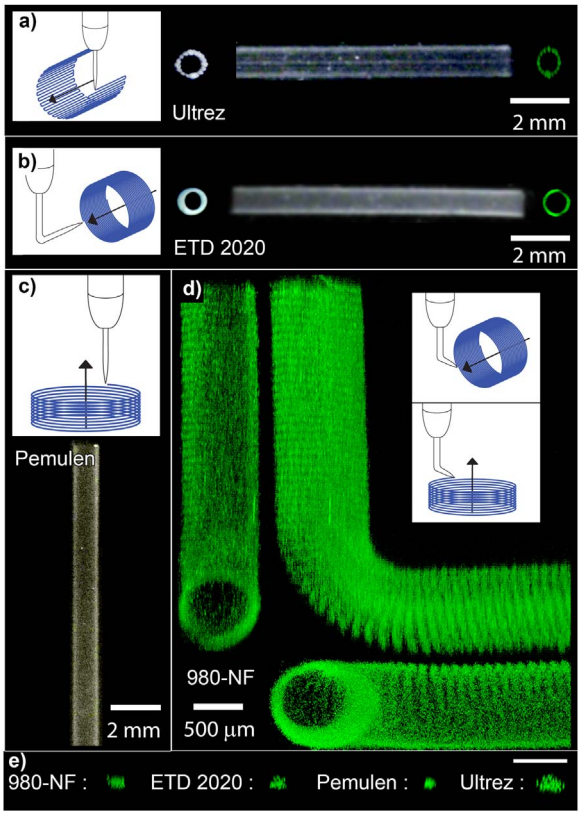

Fig. 4. Macroscopic and confocal imaging of 3D printed tubes 1 mm diameter with wall thickness of order 125 µm. (a) Horizontal orientation in Ultrez with a vertical nozzle following a layer-by-layer printing path. (b) Horizontal orientation printed into ETD 2020 with a bent nozzle and helical printing path. (c) Vertical orientation in Pemulen with a vertical nozzle following a helical printing path. (d) Confocal imaging of an "L"-shaped tube printed into 980-NF with a printing nozzle bent at 45° following a helical printing path. (e) An end-on view of single linear features printed the four microgel systems exhibit diameters ranging from 20 to 50 µm (scale 100 µm). This view of the features is generated by a maximum intensity projection along the linear feature, showing the absolute border of each written structure.

extracellular matrix is included, so these results do not necessarily indicate a lack of suitability for any of these materials for bioprinting applications [9]. However, as the use of LLS for 3D cell culturing grows, it may be necessary to develop new microgels to improve cell viability and performance in the absence of added matrix, potentially through a reduction in the polymeric charge density.

To demonstrate the potential of these commercially available microgel systems for 3D bioprinting, we print a series of horizontal, vertical, and bent tubes out of a mixture of polyvinylalcohol polymer and fluorescent microspheres (Fig. 4). Each tube is printed into a different microgel system prepared at the concentrations present in Fig. 2, using different tip designs, and path planning strategies designed to leverage the unique printing opportunities available when printing into jammed granular microgels. While it is possible to print both horizontal (Fig. 4a) and vertical tubes (Fig. 4c) with a single needle design, certain geometries are better suited for a given orientation. Structures created from continuous helical patterns (Fig. 4b) are observed to have higher degrees of cross-sectional symmetry than those printed using more complex paths (Fig. 4a). By utilizing a needle oriented at 45° from vertical, we are able to follow a continuous helical pattern in both the horizontal and vertical directions without damaging the printed structure. This tip design enables bent tubular structures to be printed in a single path without interruption (Fig. 4d). To directly test the level of precision achievable in the different microgel systems, single features are drawn and measured with confocal microscopy, demonstrating a feature size as small as 20 µm (Fig. 4e).

4. Conclusion

Here we have studied several different liquid-like solid materials made from commercially available microgels of differing chemical composition. We have found that the rheological properties of these materials can be tuned and optimized to perform similarly in 3D printing. All four systems behave like soft elastic solids at low strains, yield at low stresses, and transition rapidly between the solid and fluidized states. These rheological behaviors differ qualitatively from other complex fluids like entangled or dynamically bonding polymer networks, which exhibit apparent yielding and solid-like behaviors at short time-scales, yet evolve spontaneously over long times due to thermally driven relaxations [5]. By contrast, jammed granular microgels are thermodynamic solids and can support 3D printed structures for long times. The performance of these materials for 3D bioprinting is demonstrated by the ability to generate fine, precise structures with numerous tip designs, feature orientations, and printing paths. The ability to print tubes in arbitrary orientations, in conjunction with the ability to join tubes with complex connections opens the door to creating complex 3D tubular networks, which is a huge challenge in tissue engineering applications. While preliminary short-term cell viability studies of cells cultured in LLS are presented here, further studies of long-term cell viability and metabolic activity are needed if these microgels are to be used in bioprinting applications; the results described here demonstrate their promise in terms of rheology and printing performance.

Acknowledgements

The authors would like to thank Alberto Fernandez-Nieves and Ya-Wen Chang for helpful discussions and guidance.

Funding source

This material is based on work supported by the National Science Foundation under grant no. DMR-1352043.Author contributions

The manuscript was written through contributions from all authors. C.O. and T.B. performed the rheological measurements of the microgels. C.O., T.B., and S.M. 3D printed structures into the microgel support. T.A. and W.S. provided supervision and guidance throughout the project. All authors have given approval to the final version of this manuscript.Declaration of interests

None.

References

[1] S.V. Murphy, A. Atala, 3D bioprinting of tissues and organs, Nat. Biotechnol. 32 (2014) 773.
[2] K. Jakab, C. Norotte, F. Marga, K. Murphy, G. Vunjak-Novakovic, G. Forgacs, Tissue engineering by self-assembly and bio-printing of living cells, Biofabrication 2 (2010) 022001.
[3] C.J. Ferris, K.J. Gilmore, S. Beirne, D. McCallum, G.G. Wallace, Bio-ink for on-demand printing of living cells, Biomater. Sci. 1 (2013) 224–230.
[4] A.L. Rutz, P.L. Lewis, R.N. Shah, Toward next-generation bioinks: tuning material properties pre-and post-printing to optimize cell viability, MRS Bull. 42 (2017) 563–570.
[5] C.S. O'Bryan, T. Bhattacharjee, S.R. Niemi, S. Balachandar, N. Baldwin, S.T. Ellison, et al., Three-dimensional printing with sacrificial materials for soft matter manufacturing, MRS Bull. 42 (2017) 571–577.
[6] D. Williams, P. Thayer, H. Martinez, E. Gatenholm, A. Khademhosseini, A perspective on the physical, mechanical and biological specifications of bioinks and

the development of functional tissues in 3D bioprinting, Bioprinting (2018).
[7] S.E. Bakarich, R. Gorkin III, M. in het Panhuis, G.M. Spinks, Three-dimensional printing fiber reinforced hydrogel composites, ACS Appl. Mater. Interfaces 6 (2014) 15998–16006.
[8] S. Hong, D. Sycks, H.F. Chan, S. Lin, G.P. Lopez, F. Guilak, et al., 3D printing of highly stretchable and tough hydrogels into complex, cellularized structures, Adv. Mater. 27 (2015) 4035–4040.
[9] T. Bhattacharjee, C.J. Gil, S.L. Marshall, J.M. Urueña, C.S. O'Bryan, M. Carstens, et al., Liquid-like solids support cells in 3D, ACS Biomater. Sci. Eng. 2 (2016) 1787–1795.
[10] T. Bhattacharjee, S.M. Zehnder, K.G. Rowe, S. Jain, R.M. Nixon, W.G. Sawyer, et al., Writing in the granular gel medium, Sci. Adv. 1 (2015) e1500655.
[11] C.S. O'Bryan, T. Bhattacharjee, S. Hart, C.P. Kabb, K.D. Schulze, I. Chilakala, et al., Self-assembled micro-organogels for 3D printing silicone structures, Sci. Adv. 3 (2017) e1602800.
[12] T.J. Hinton, Q. Jallerat, R.N. Palchesko, J.H. Park, M.S. Grodzicki, H.-J. Shue, et al., Three-dimensional printing of complex biological structures by freeform reversible embedding of suspended hydrogels, Sci. Adv. 1 (2015) e1500758.
[13] D.F. Evans, H. Wennerstrom, Colloidal Domain, Wiley-Vch, New York, 1999.
[14] Carbopol Polymer Products. ⟨https://www.lubrizol.com/Life-Sciences/Products/Carbopol-Polymer-Products⟩. (Accessed 1 October 2018).
[15] J.L.I. Carl, Z. Amjad, W.F. Masler III, W.H. Wingo, Easy to disperse polycarboxylic acid thickeners. US005288814A, issued, 1994.
[16] Pemulen Polymeric Emulsifiers. ⟨https://www.lubrizol.com/Life-Sciences/Products/Pemulen-Polymeric-Emulsifiers⟩. (Accessed 1 October 2018).
[17] A.A. Guerrero, A. Vargas, Cosmetic composition containing emulsifying copolymer and anionic sulfosuccinate. US005236710A, issued, 1993.
[18] T. Bhattacharjee, C.P. Kabb, C.S. O'Bryan, J.M. Urueña, B.S. Sumerlin, W.G. Sawyer, et al., Polyelectrolyte scaling laws for microgel yielding near jamming, Soft Matter 14 (2018) 1559–1570.
[19] W.H. Herschel, R. Bulkley, Konsistenzmessungen von gummi-benzollösungen, Colloid Polym. Sci. 39 (1926) 291–300.